Supporting Information: Electrocatalytic Reduction Mechanisms of CO_2 on MoS_2 Edges using Grand-Canonical DFT: from CO_2 Adsorption to HCOOH or CO

Muhammad Akif Ramzan,[†] Rémi Favre,[‡] Stephan N. Steinmann,[*,‡] Tangui Le Bahers,[*,‡,¶] and Pascal Raybaud[*,†,‡]

†*IFP Energies nouvelles, Rond-point de l'échangeur de Solaize - BP 3 69360 Solaize - France*

‡*CNRS, Laboratoire de Chimie UMR 5182, ENS de Lyon, 46 allée d'Italie, Lyon F-69342, France*

¶*Institut Universitaire de France, 5 rue Descartes, 75005 Paris, France*

E-mail: stephan.steinmann@ens-lyon.fr; tangui.le_bahers@ens-lyon.fr; pascal.raybaud@ifpen.fr

Contents

S1 Hydrogenation of Mo/S edges

As a first step, we investigated the stable edge structures resulting from potential-induced hydrogenation of the two edges: readily-available H^+ in the electrolyte can adsorb on the surface of the catalyst. To this end, we define the following quantity akin to surface free energy,

$$\Delta G^{nH}(U) = \left(G^{nH}(U) - n \times G\left(H^+ + e^-\right) \right) - G_{ref}(U), \tag{S1}$$

where $G^{nH}(U)$ is the potential-dependent Gibbs free energy of the simulated supercell with 'n' H atoms adsorbed on the given edge and $G_{ref}(U)$ is the potential-dependent free energy of an arbitrary reference structure. The second quantity in parenthesis in Eq. S1 is the free energy of a proton-electron pair which, at standard conditions, is in equilibrium with gaseous H_2. Therefore, according to the Nørskov's approach,[S1] this quantity is defined as

$$G\left(H^+ + e^-\right) = \frac{1}{2} G_{H_2} - eU, \tag{S2}$$

where G_{H_2} is the Gibbs free energy of H_2 in the gas phase at standard conditions, e the elementary charge and U is the applied electrode potential, all in suitable units. In the context of HER, Eq. S1 can be considered as cumulative energy change of 'n' Volmer steps. It is worth noting that the CHE approach also incorporates Eq. S2 for posteriori inclusion of potential dependence. However, it doesn't explicitly account for the potential dependence present in $G^{nH}(U)$ and $G_{ref}(U)$.

S1.1 S-edge

The S-edge exposes four-fold Mo atoms bonded to two-fold S atoms in a zigzag fashion. First H on this edge is preferentially adsorbed between two Mo atoms in a bridge position (Figure S2(a)), in line with previous theoretical studies,[S2] instead of adsorbing on S atom, as proposed in ref.[S3] Notably, S-edge does not undergo any significant reconstruction upon relaxation (Figure S1), therefore, the four Mo−Mo sites were deemed equivalent for the adsorption of first H. This preference for

Mo−H−Mo adsorption continues up to 0.5 ML coverage with successive H's adsorbing closer to the previously adsorbed H atoms (Figure S2(b)). Beyond 0.5 ML, H is adsorbed at S with successive H's adsorbing farther from the previously formed S−H moiety.

Using Eq. S1, the Volmer phase diagram obtained for the hydrogenation of S-edge as a function of electrode potential is given in Figure S3(a). We observe the strong tendency of S-edge to hydrogenate: even at 0 V, the S-edge is already covered with 0.5 ML H. The half-monolayer coverage remains the most stable edge-structure up to -0.45 V after which the full-monolayer coverage becomes the most stable phase.

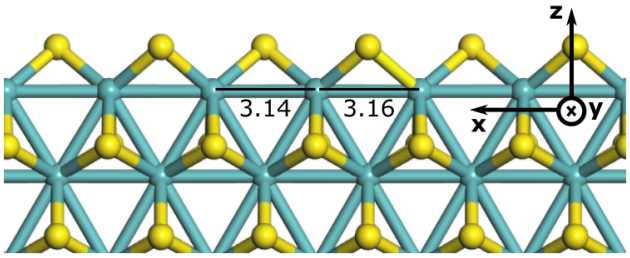

Figure S1: Mo−Mo distances in Å for the topmost Mo atoms exposed on fully relaxed bare S-edge.

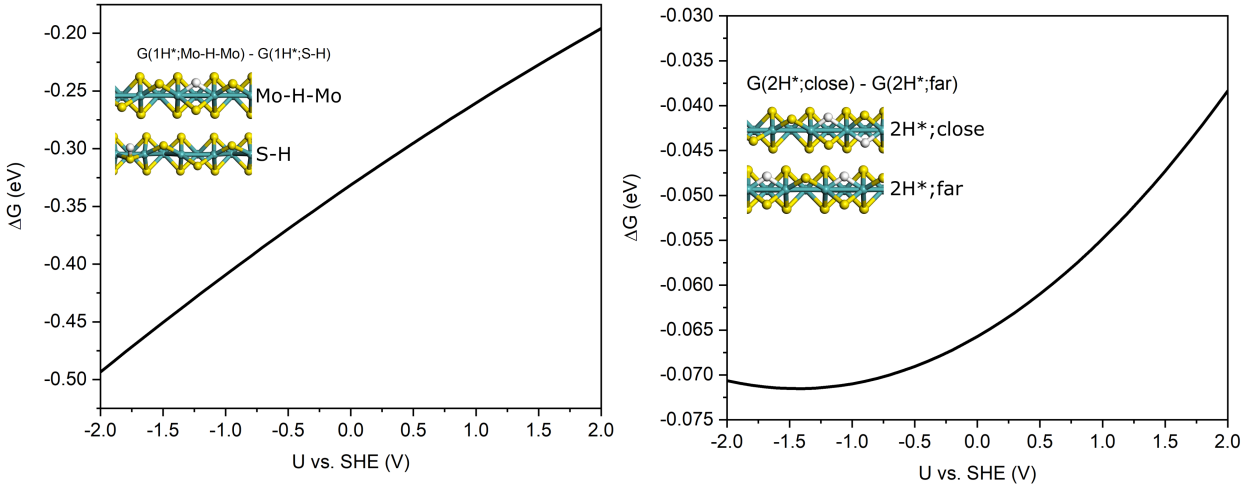

Figure S2: Comparison of the relative stability of two possible adsorption configurations for(a) 0.125 ML and (b) 0.25 ML H on S-edge.

In Figure S4(a) we plot the Volmer and Heyrovsky reaction free energies at each coverage for two electrode potentials of interest (in Figure S5(a), we plot their evolution over the full potential

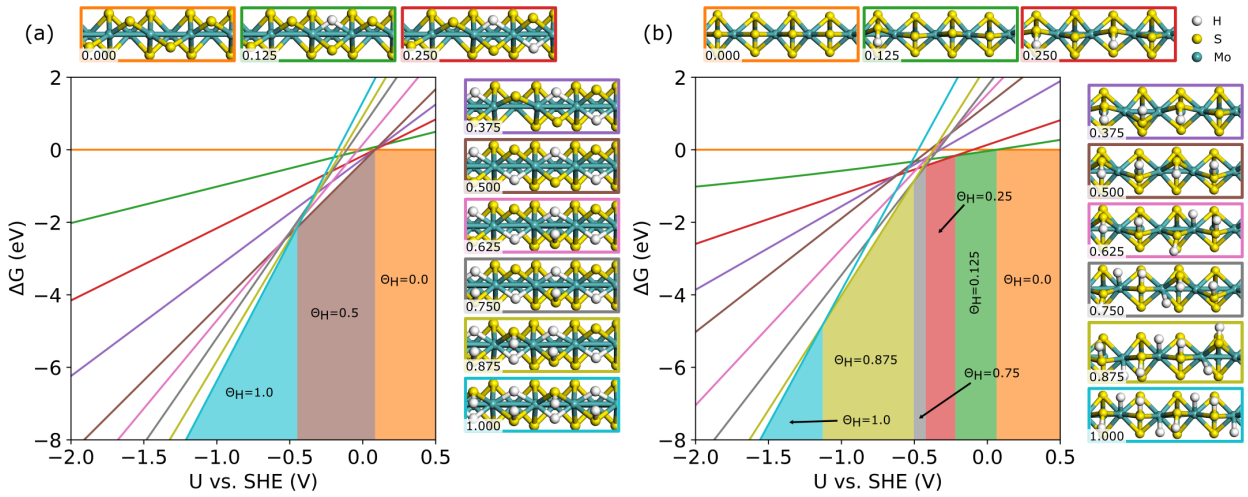

Figure S3: Volmer phase diagram for the hydrogenation of (a) S-edge and (b) Mo-edge as a function of electrode potential and the corresponding most-stable, zero-charge-optimized adsorption geometries for each coverage. The colors of the plots correspond to the colors of the boxes around the structures.

range). We notice that at low coverages, the Volmer step is always more exergonic than Heyrovsky leading to an accumulation of H atoms on the S-edge. However, at 0.5 ML we observe a reversal in the relative Volmer and Heyrovsky reaction energies. For all subsequent coverages, the Heyrovsky step is more exergonic than the corresponding Volmer step at all potentials. This suggests that even though higher coverages are thermodynamically accessible at higher reducing potentials, corroborated, for example, by the negative ΔG_{Vol} values for all coverages at -0.6 V, they are expected to be destabilized due to highly exergonic Heyrovsky step at those potentials: any additional H beyond 0.5 ML coverage is readily evolved into gaseous H_2. Indeed, the largest difference ($\Delta G_{Hey} - \Delta G_{Vol}$) is observed at 0.625 ML indicating that the 5^{th} H, which forms an S−H moiety, is very unstable on the surface and would easily form H_2 via Heyrovsky mechanism. Consequently, 0.5 ML can be considered as the equilibrium, steady-state coverage, even at highly reducing potentials. This reveals that the Volmer phase diagram (Figure S3) is not sufficient to capture the thermodynamic stability of edge species due to potential competition from Heyrovsky.

Based on Figure S4(a), we remark that at 0 V, which corresponds to the conditions generally employed for HER, S-edge shows H adsorption close to zero (ΔG_{Vol}@0.375ML = -0.09 eV),

which should make it highly active for HER. The potential dependence of this Volmer step (ΔG_{Vol}@0.375ML in Figure S5(a)) reveals that it is a true PCET step amounting to a transfer of 1 electron. Conversely, at -0.6 V, although H is very strongly adsorbed with ΔG_{Vol}@0.375 ML = -0.70 eV, however, the corresponding Heyrovsky step is also highly exergonic (ΔG_{Hey}@0.5 ML = -0.50 eV at 0.5 ML) which could still lead to the evolution of H_2.

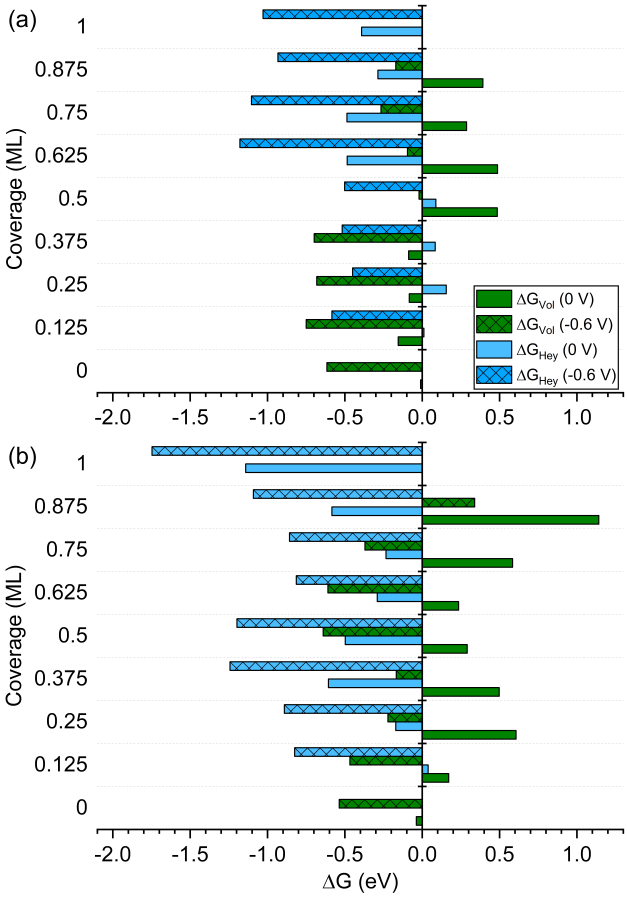

Figure S4: Volmer and Heyrovsky reaction free energies as a function of coverage on (a) S-edge and (b) Mo-edge at two relevant potentials of interest, U = 0 V and U = -0.6 V.

S1.2 Mo-edge

Similar to S-edge, we studied the Volmer phase diagram on Mo-edge (Figure S3(b)) which is characterized by six-fold Mo atoms bonded to two-fold S atoms. Unlike S-edge, the first H preferentially binds to the S atom on Mo-edge. In particular, we noticed that Mo-edge experiences significant reconstruction upon relaxation and, similar to the behavior discussed in Refs.,[S4,S5] Mo atoms cluster together in groups of two with alternating short and long Mo−Mo distances. In turn, adsorption of H is preferred, by ≈ 0.4 eV, on the S bonded to Mo atoms which are farther apart (Figure S6). This preference for S−H binding continues up to 0.5 ML. The 0.25 ML coverage contains two *cis*-oriented S−H moieties located one atom apart (Figure S7), in line with previous theoretical studies.[S6] In terms of the phase diagram, Mo-edge displays many different zones of stability corresponding to increasing H coverage as the electrode potential becomes more reducing. Similar to S-edge, hydrogenation of the Mo-edge can take place even before 0 V, however, the H coverage stays low (0.125 ML compared to 0.5 ML on S-edge). For potentials lower than -0.22 V, we first observe a gradual increase of coverage to 0.25 ML which is followed by a sudden jump to 0.75 ML coverage at -0.42 V. Finally, around -0.50 V we see a large stability zone of 0.875 ML coverage, which is eventually overtaken by full-monolayer coverage around -1.1 V.

Similar to the S-edge, the adsorption free energy of H (first H) on Mo-edge is -0.04 eV at 0 V which reinforces the notion that the Mo-edge is also catalytically active for HER, as substantiated by previous theoretical and experimental studies.[S7,S8] However, in contrast to S-edge, the weak potential dependence observed for this initial Volmer step suggests a partially decoupled proton-electron transfer (Figure S5(b)), involving the transfer of approximately 0.5 electrons. In other words, this step should be interpreted as occurring somewhere between the processes of protonation and hydrogenation of the Mo-edge. Conversely, at -0.6 V, both Volmer and Heyrovsky steps are highly exergonic which should still render this edge high HER activity at typical conditions of CO_2 reduction.

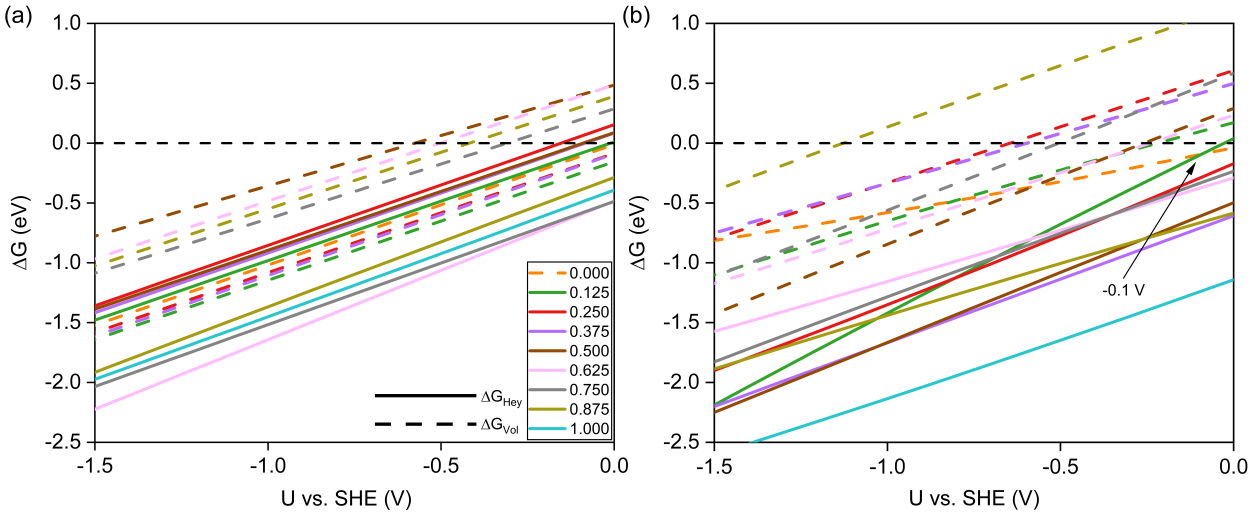

Figure S5: Volmer and Heyrovsky reaction free energies as a function of electrode potential for all coverages investigated on (a) S-edge and (b) Mo-edge.

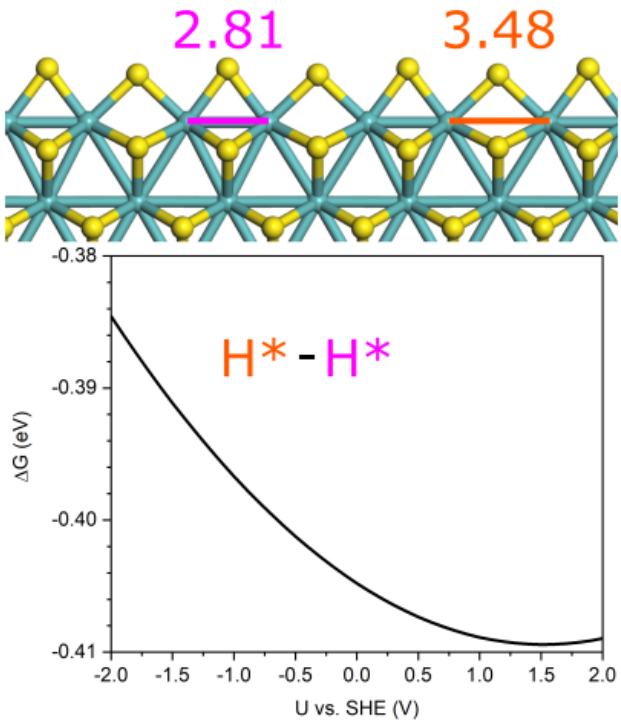

Figure S6: Difference of the GC free energy of two adsorption configurations for 0.125 ML H on Mo-edge; H prefers to adsorb on the S atom that is connected to Mo atoms which are farther apart. The top inset shows Mo−Mo distances in Å.

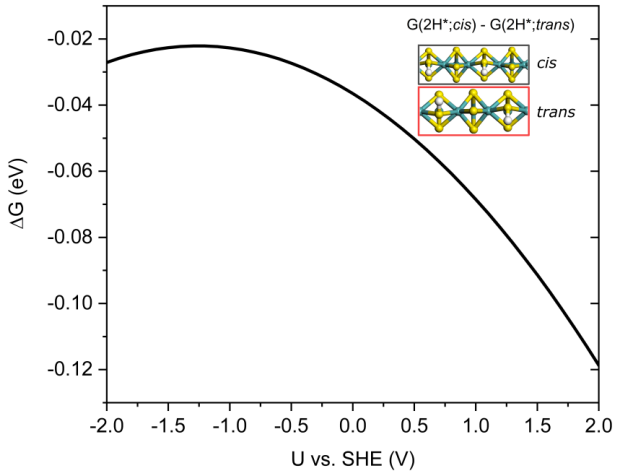

Figure S7: Comparison of the relative stability of two possible adsorption configurations for 0.25 ML H on Mo-edge of the MoS_2. The *cis*-adsorbed S−H moities are more favorable as previously shown by computations.[S6]

S2 CO_2 activation *via* adsorption

S2.1 S-edge

Different adsorption modes of CO_2 were tested on the S-edge. In Figure S8 we plot the GC free energy as a function of electrode potential for the three most-stable adsorption modes on bare S-edge. The VdW mode involving only a physical interaction with the MoS_2 edges is overtaken by the Mo-Mo adsorption mode even before 0 V. Therefore, we do not study VdW mode for more realistic cases where S-edge has coadsorbed H. The Mo-S mode was also found to be less stable than Mo-Mo mode even though it causes no reconstruction of the S-edge unlike Mo-Mo mode where a S monomer is displaced from its most stable zigzag configuration. The difference in stability of Mo-Mo and Mo-S adsorption modes was even greater in the presence of H. Thus we only focus on the Mo-Mo adsorption mode and study its coadsorption with H as discussed in the main text.

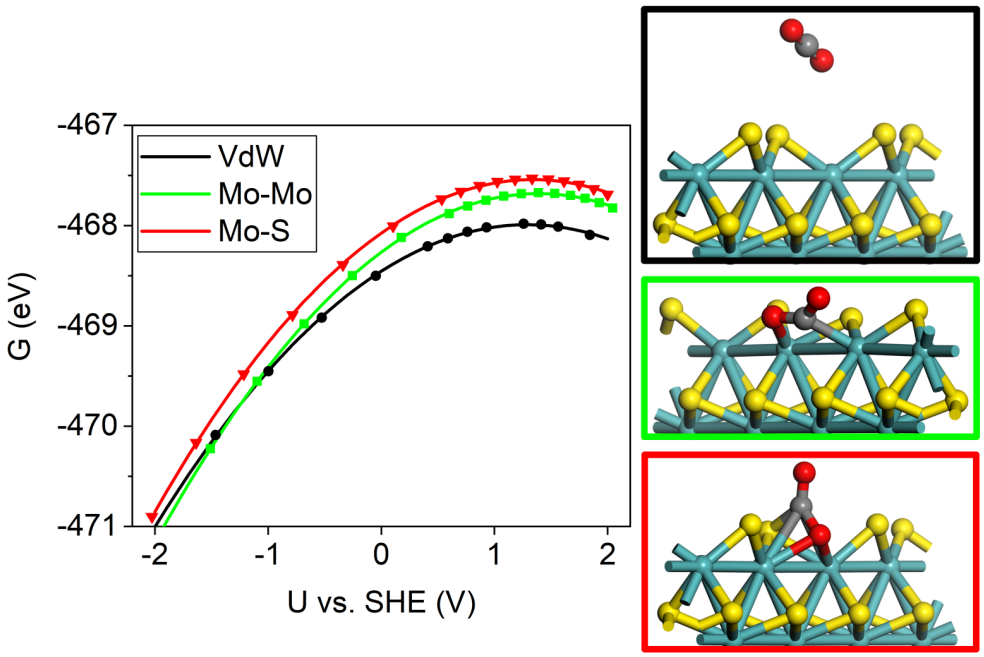

Figure S8: Extrapolation curves of the GC free energy for three different adsorption modes of CO_2 on bare S-edge. The symbols represent the actual DFT-obtained GC energies while lines are the corresponding parabolic fit.

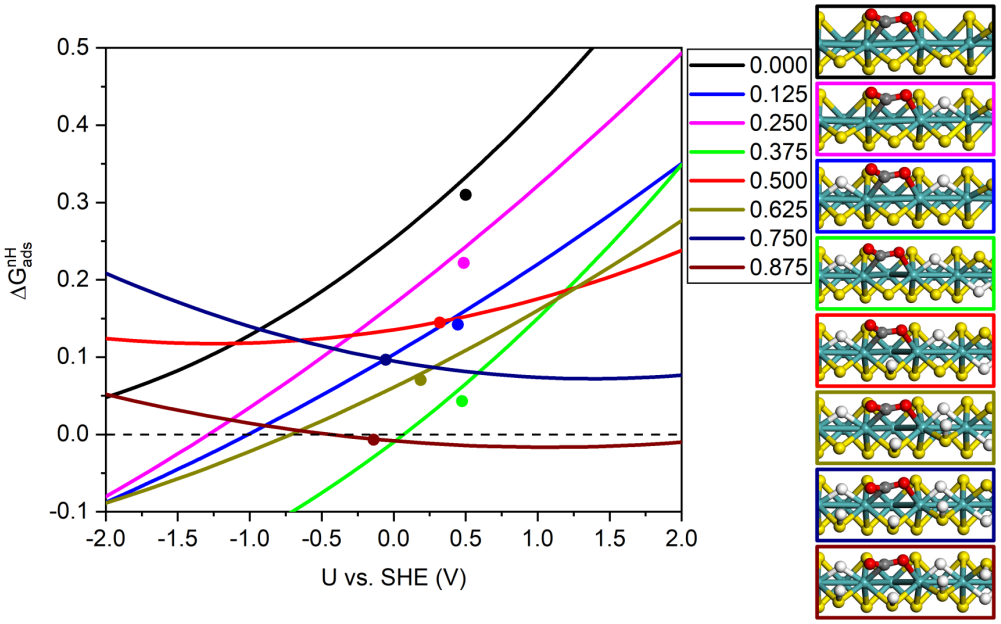

Figure S9: Adsorption free energy of Mo-Mo adsorption mode of CO_2 on S-edge as a function of electrode potential and H coverage from 0.0-0.875 ML, the maximum coverage of H possible in coadsorption with CO_2^*. The filled circles correspond to the potential of zero charge for the coadsorbed system and the corresponding adsorption free energy of the neutral systems.

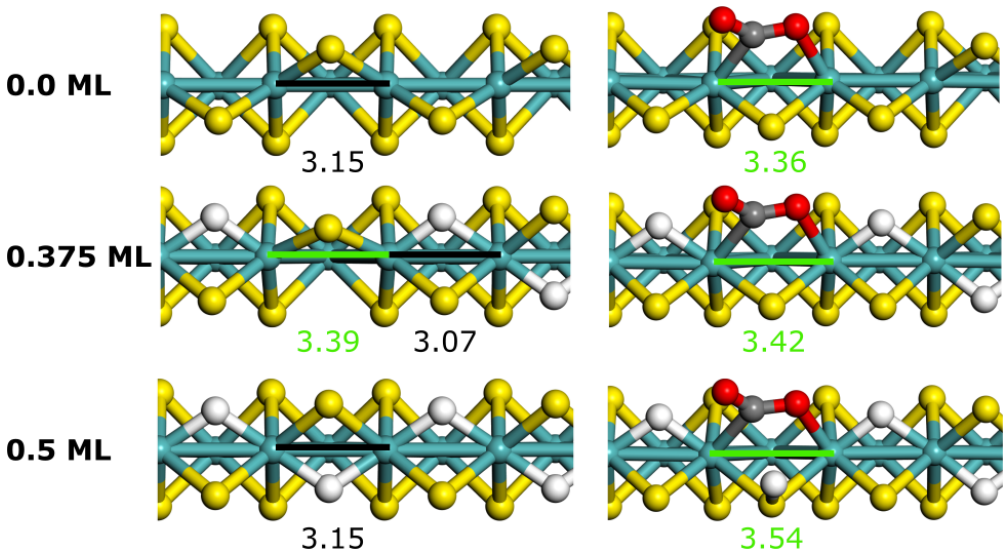

Figure S10: Comparison of the Mo−Mo distances (Å) before and after CO_2 adsorption on S-edge for three H coverages on S-edge.

S2.1.1 Electronic analysis for adsorption of CO_2 on S-edge

Bader charge analysis was performed and the corresponding net atomic charges are given in Table S1. If we first consider the electronic behavior of the atoms located on the S-edge in absence of CO_2, we notice that the Mo atoms are all positively charged. Thus H1, H2, H3 atoms bridging between Mo atoms have hydride characters; H4 is negatively charged (hydride character) in the reference 'edge' state but is positively charged (protonic character) in the coadsorbed system due to its bonding with the electronegative S atom. The corresponding S atom becomes less-negatively charged in the coadsorbed state as it loses its electronic density to H4 atom. The positive charges of the Mo-atoms increase with H coverage. In presence of adsorbed CO_2, the charges of Mo1 and Mo2 atoms interacting with CO_2 become significantly more positive (0.24e). At the same time, the charge of the CO_2 molecule becomes negative (-0.87e). This negative charge is distributed on both the C and O atoms, with a significant charge fluctuation on the C atom. It is worth noting that, as is the case in the gas phase, both O atoms in the adsorbed CO_2^* state have similar charges, even though one is *bonded* to Mo and the other one is *free*. This further highlights the redistribution of the charge that is conferred from the surface to the CO_2 molecule.

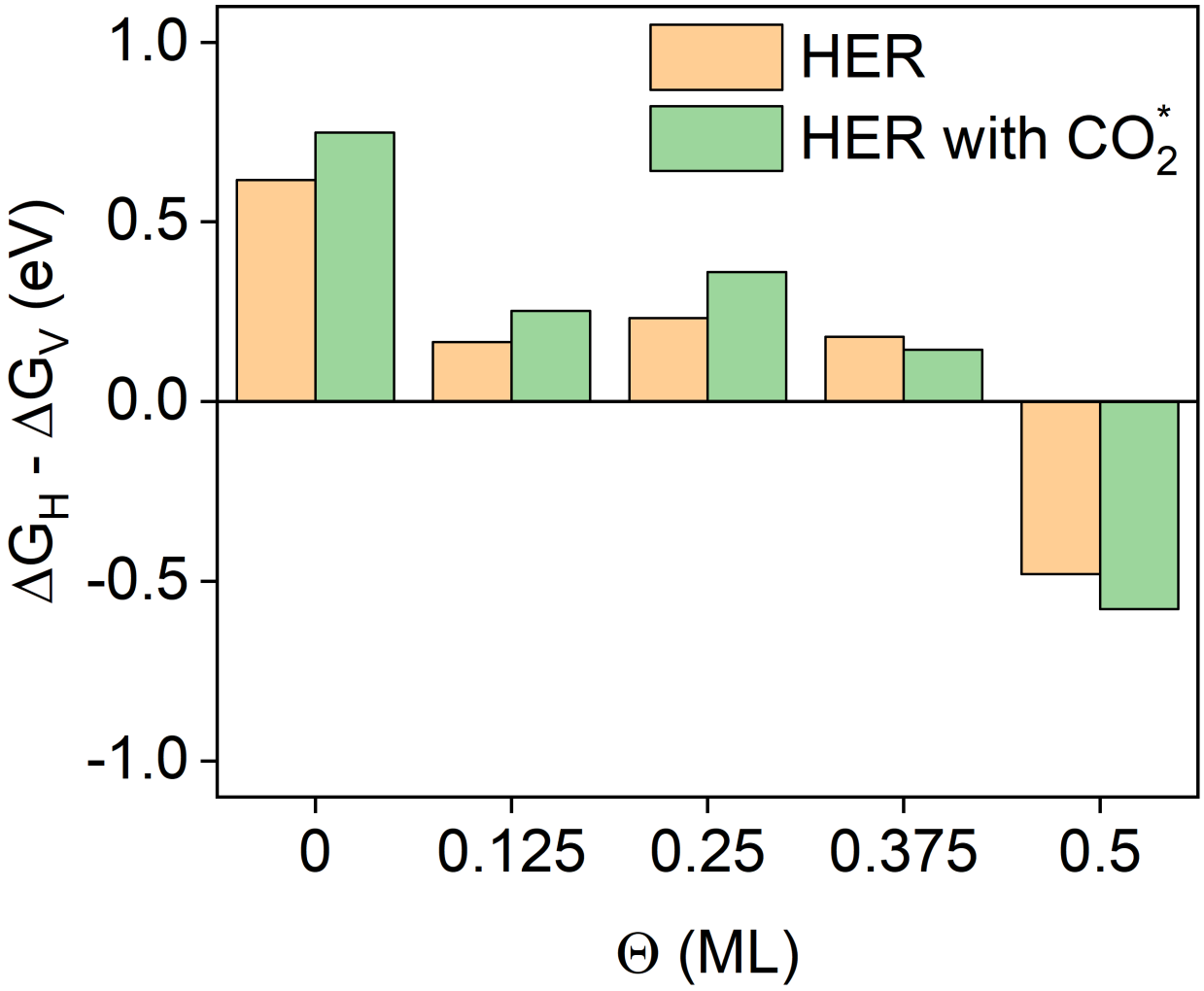

Figure S11: Difference of Heyrovsky and Volmer Gibbs free energy change for the H/CO_2@S-edge coadsorbed system as a function of H coverage at -0.6 V.

The charged case for 0.375 ML coverage shows well-distributed charge over the whole system. The charging mainly helps the surface recover back its electronic density which was extracted by the adsorbed CO_2 molecule. This makes the surface and, in turn the whole coadsorbed system, more stable

Table S1: Bader atomic charges for relevant atoms which are highlighted in the inset at the bottom. 'slab' structure corresponds to the most stable edge structure at that coverage, show in Figure 2(a). The charges were computed *via* a single point calculation, on top of the PBE+D3 optimized geometries, using range separated hybrid functional HSE06[S9] and gamma point for Brillouin zone sampling. The charged configuration for 0.375 ML corresponds to -1.57e, which is equivalent to a potential of -0.8 V.

	CO_2	0.0 ML		0.375 ML			0.5 ML	
	Gas phase	edge	CO_2*	edge	CO_2* neutral	CO_2* charged	edge	CO_2*
Mo1	-	1.139	1.307	1.189	1.384	1.361	1.230	1.332
Mo2	-	1.136	1.224	1.192	1.288	1.267	1.233	1.239
Mo3	-	1.138	1.112	1.210	1.246	1.210	1.230	1.204
Mo4	-	1.136	1.114	1.214	1.245	1.211	1.232	1.202
S1	-	-0.723	-0.549	-0.691	-0.615	-0.664	-0.633	-0.368
S2	-	-0.723	-0.655	-0.588	-0.596	-0.664	-0.633	-0.610
S3	-	-0.724	-0.630	-0.587	-0.581	-0.645	-0.633	-0.595
S4	-	-0.724	-0.682	-0.597	-0.609	-0.684	-0.633	-0.599
H1	-	-	-	-0.279	-0.278	-0.291	-0.320	-0.268
H2	-	-	-	-0.279	-0.293	-0.304	-0.320	-0.281
H3	-	-	-	-0.302	-0.301	-0.308	-0.321	-0.293
H4	-	-	-	-	-	-	-0.321	0.074
O	-1.089	-	-1.144	-	-1.133	-1.171	-	-1.167
C	2.177	-	1.492	-	1.486	1.471	-	1.455

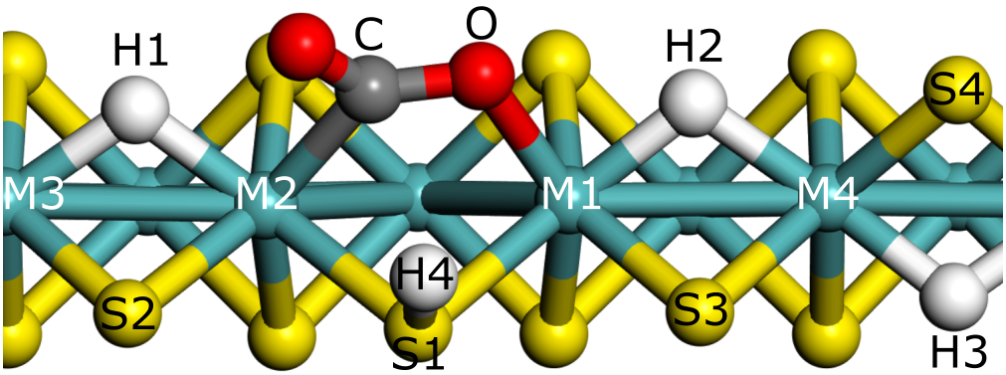

S2.2 Mo-edge

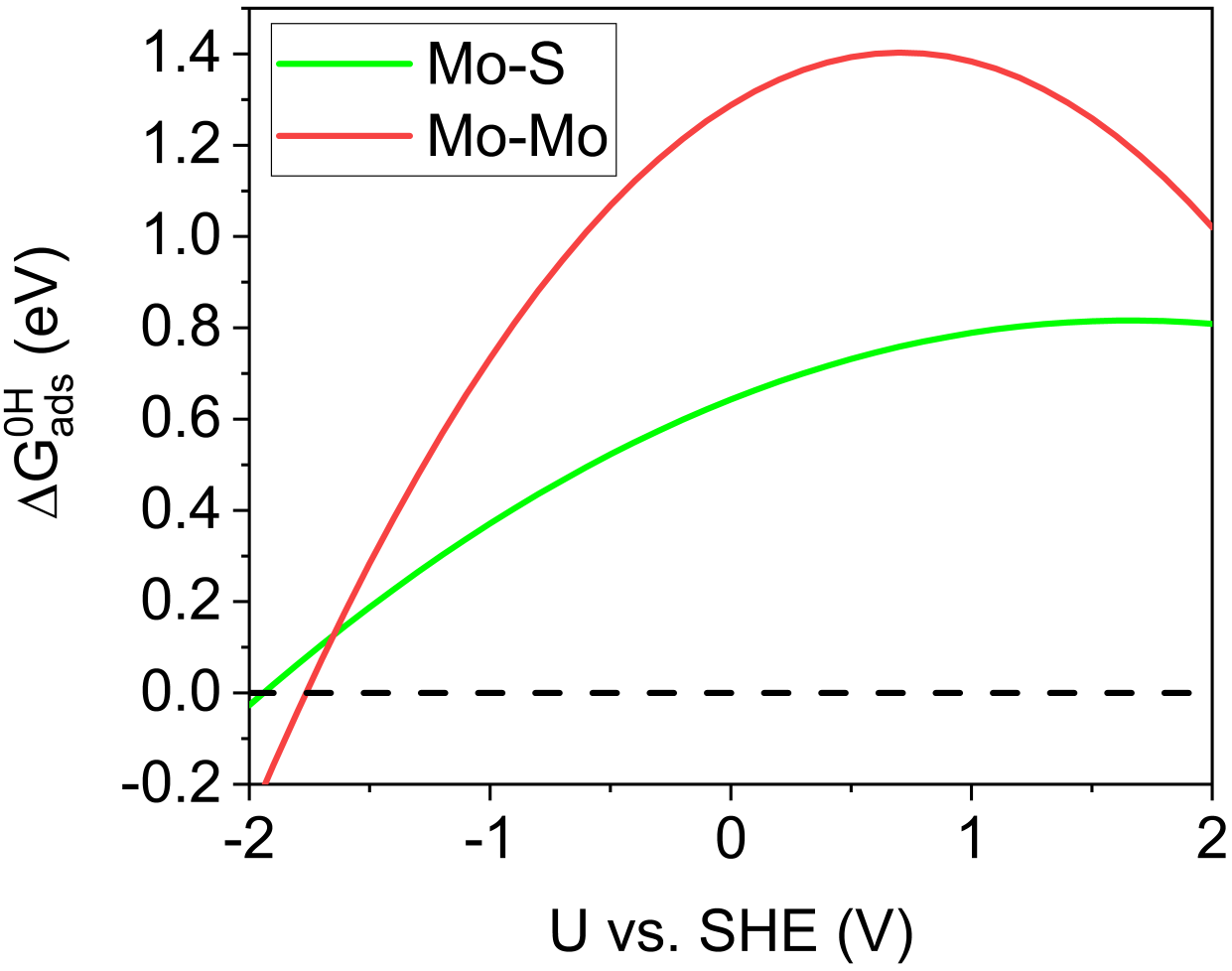

Figure S12: Free energy change of adsorption for two different adsorption modes of CO_2 as a function of electrode potential on bare Mo-edge.

S3 Reactivity of Mo/S edges

S3.1 Reactivity of bare edges

We have studied the reactivity of bare Mo-/S-edge as a reference case to contrast with the more general scenario where those edges have non-zero coverage of coadsorbed H under equilibrium, steady-state conditions.

S3.1.1 S-edge

In Figure S13 we plot the extrapolated GC free energy of relevant reaction intermediates on bare S-edge. To precise, by "bare" Mo-/S-edge we mean the case with no coadsorbed H atoms on either of the two edges simultaneously exposed in the simulated supercell (Figure 1). Based on

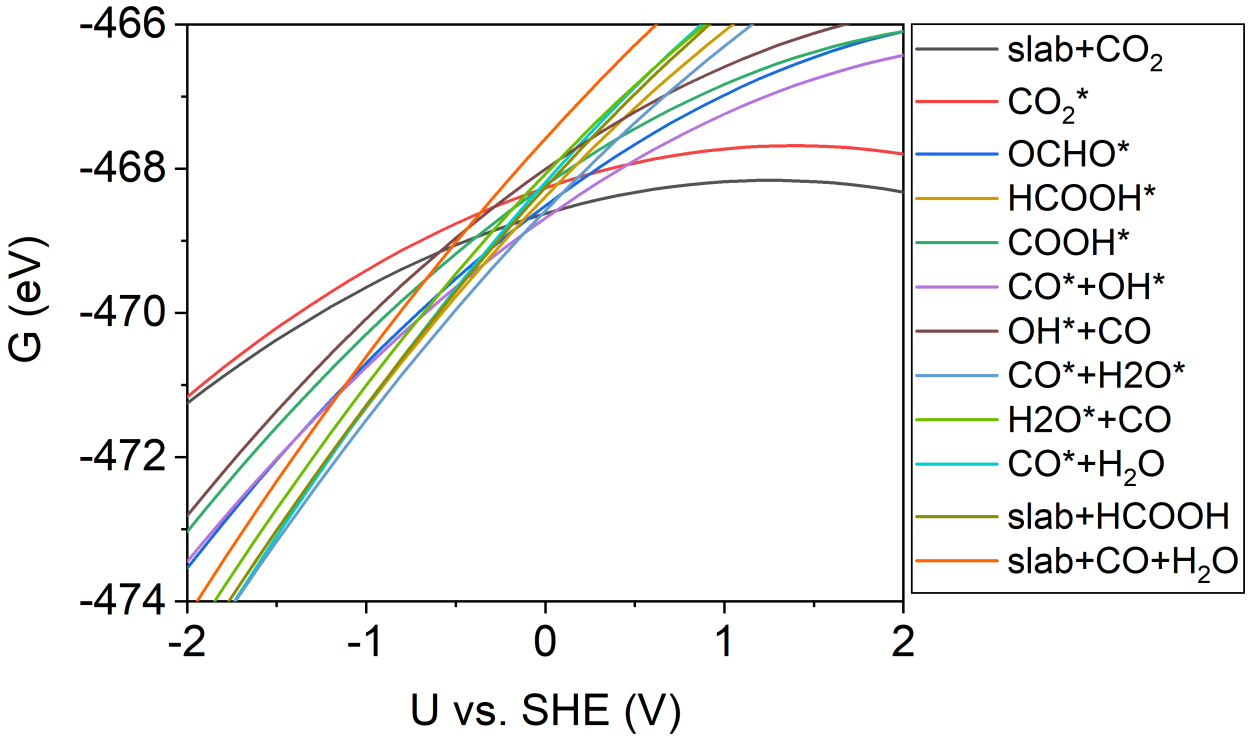

Figure S13: Extrapolated GC free energy of various reaction species studied on bare S-edge as a function of electrode potential. The adsorption geometries of the reaction intermediates are given in Figure S14.

the extrapolation curves, we plot the corresponding reaction free energy profile for bare S-edge in

Figure S14. As discussed in the main, CO_2 adsorption is not possible on this edge configuration with no coadsorbed H, signified by the high energy of CO_2^* intermediate (0.29 eV in Figure S14). We, therefore, assuming a coupled hydrogenation plus adsorption mechanism for CO_2 activation, plot the reaction profile at at -0.54 V which corresponds to the maximum reducing potential required for the optimal activity of realistic hydrogen-covered S-edge. The reactivity of this reference, bare S-edge suffers from bottlenecks involving predominantly the desorption of final products which are more strongly adsorbed in the absence of any coadsorbed H. The effect is especially pronounced for desorption of H_2O, which is exergonic on the 0.375 ML H-covered edge.

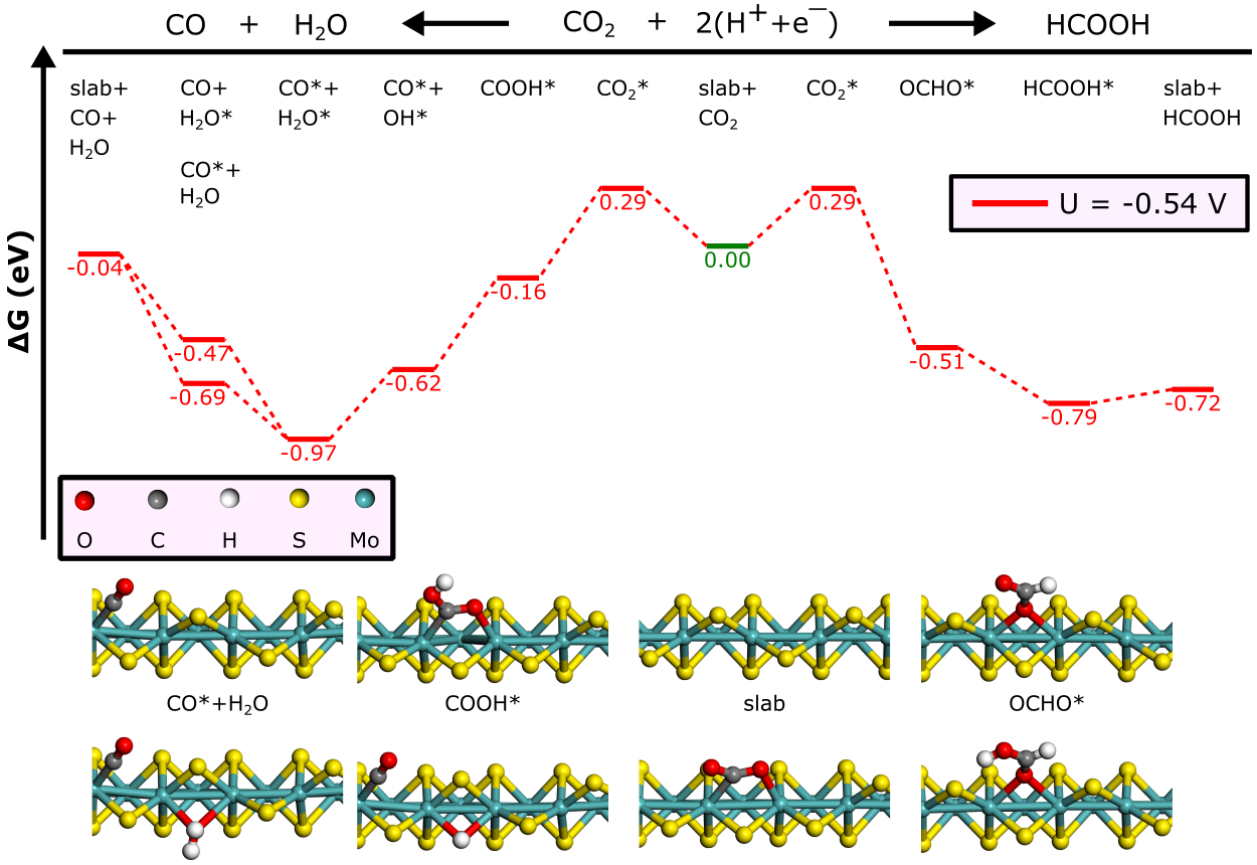

Figure S14: Free energy profile for the transformation of CO_2 into HCOOH (rightward from center) and CO (leftward from center) on bare S-edge at two electrode potentials corresponding to the alignment of $OCHO^*$ (-0.15 V) and $COOH^*$ (-0.62 V) intermediates with the reference state i.e. slab+CO_2.

S3.1.2 Mo-edge

In Figure S15 we plot the extrapolation curves for relevant intermediates found on bare Mo-edge. It is evident from this graph that CO^*+OH^* is particularly unstable on this edge hinting at the difficulty to break C−O bond. This is in line with the high coordination number of edge Mo atoms which are unable to stabilize the CO^* intermediate. CO_2 activation was also found impossible on this edge, as discussed in detail in the main text, necessitating a coupled mechanism at the start of the reaction. Another interesting difference from the bare S-edge is the comparable stability of first two reaction intermediates $OCHO^*$ $COOH^*$.

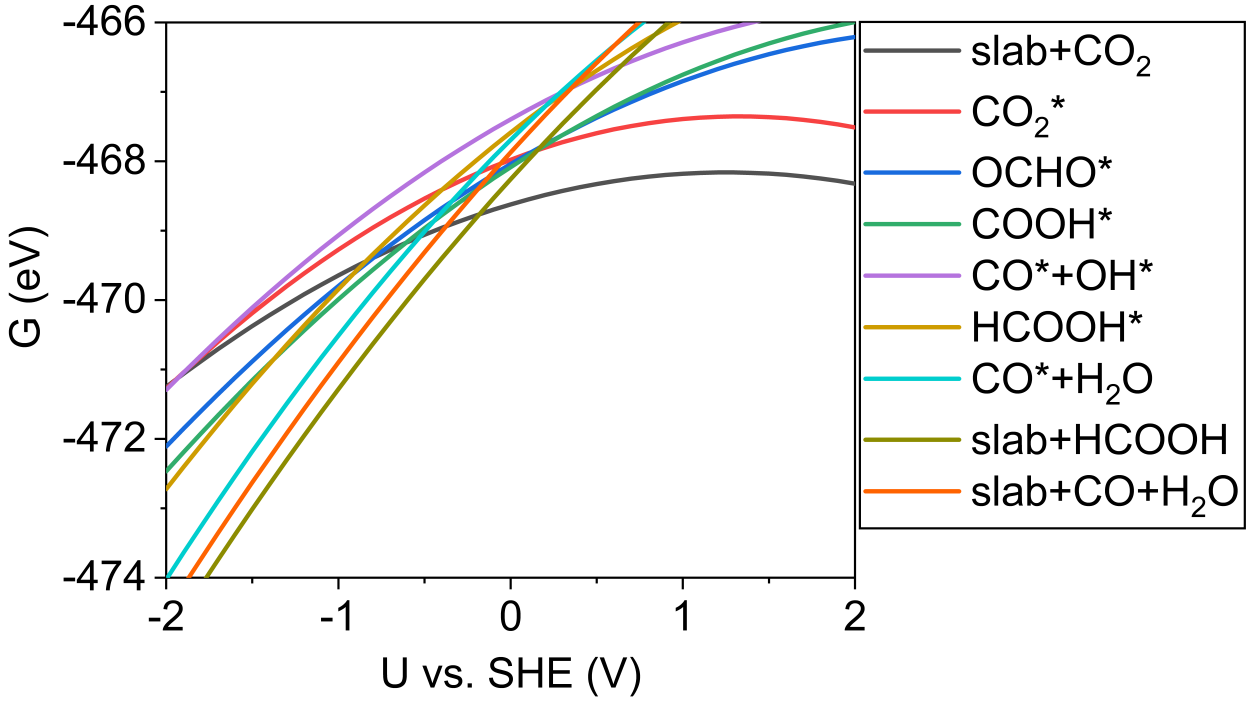

Figure S15: Extrapolated GC free energy of various reaction species studied on bare Mo-edge as a function of electrode potential.

S3.2 Reactivity of S-edge at 0.375 ML H coverage

In Figure S16 we plot the extrapolated GC free energy of the relevant reaction species for the case where S-edge is covered with 0.375 ML H. The corresponding reaction profile and the optimized geometries of the reaction intermediates are shown and discussed in the main text.

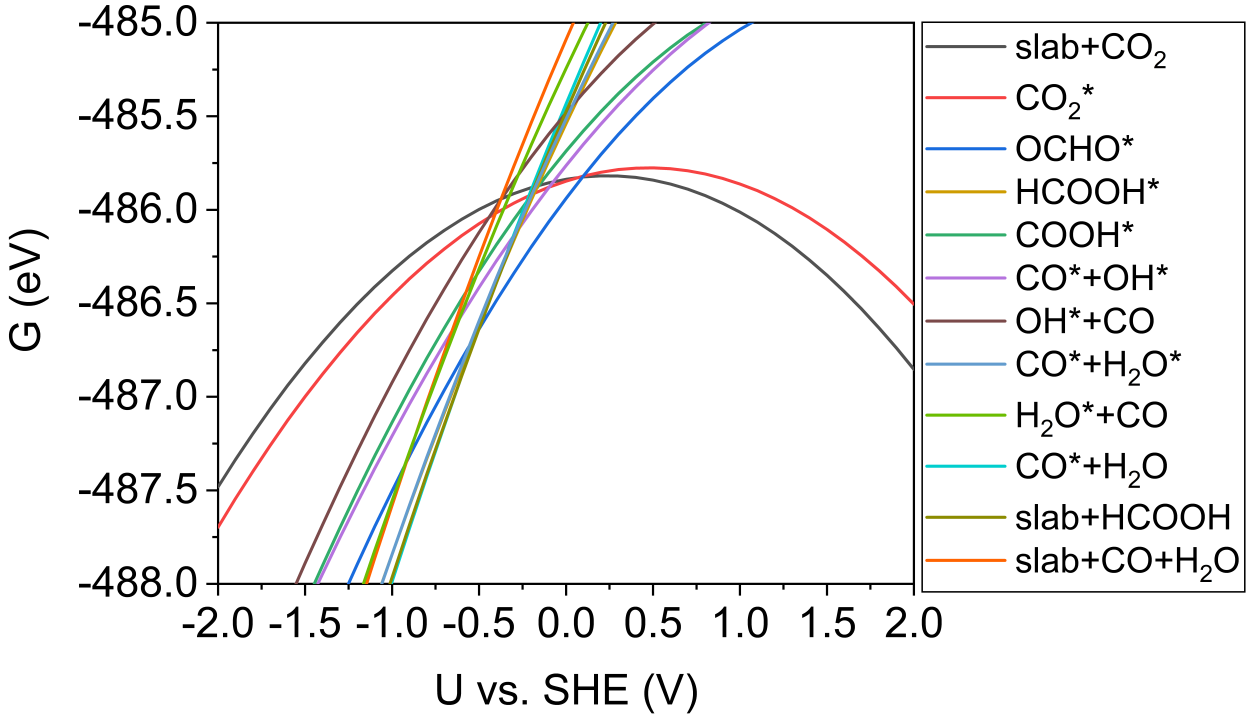

Figure S16: Extrapolated GC free energy of various reaction species on 0.375 ML H-covered S-edge as a function of electrode potential.

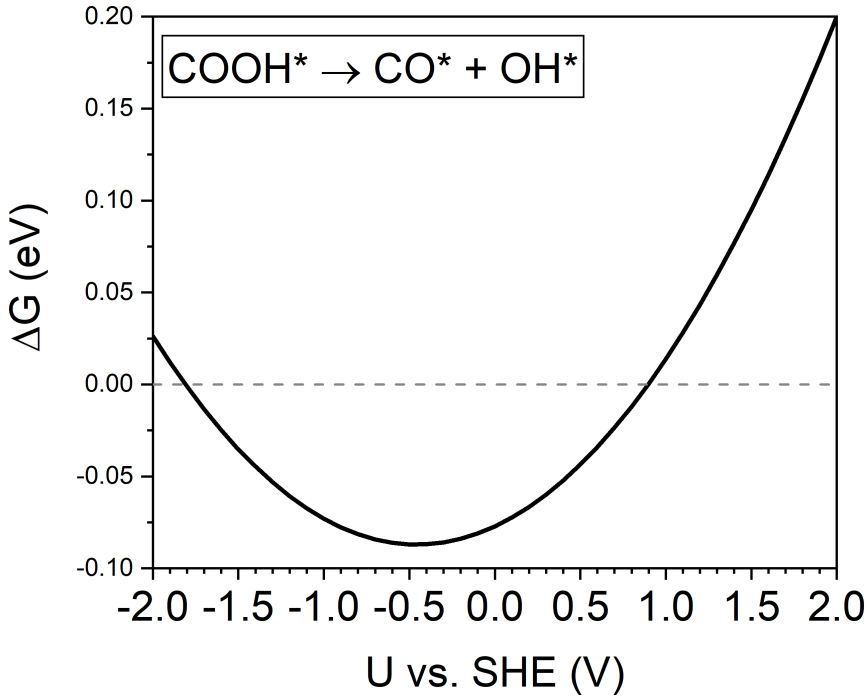

Figure S17: Free energy change of C−O bond breaking on 0.375ML H-covered S-edge. It corresponds to the free energy change of the reaction written on the plot whereas CO* and OH* are coadsorbed in the same supercell.

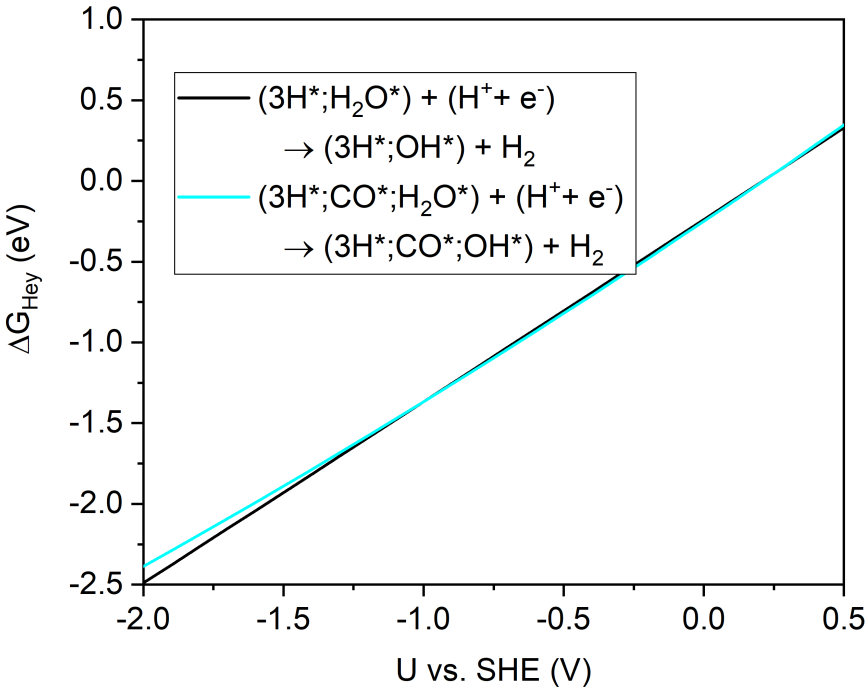

Figure S18: Free energy change of H_2 evolution via Heyrovsky step involving a $H_2O^* \longleftrightarrow OH^*$ cycle both with and without coadsorbed CO^*.

S4 Desorption of CO

MoS_2 has been shown to produce CO from (electro-)photocatalytic reduction of CO_2. However, our reactivity analysis shows that CO is very strongly adsorbed on the surface making its normal desorption very unlikely. Alternate mechanism has been proposed in the literature to understand the desorption of CO which requires a higher coverage of CO on the surface caused, in turn, by its facile diffusion.[S10] In Figure S19 we show that diffusion (black curve) is much more likely than desorption (red curve) which would result in higher coverage of CO on the surface. The optimized geometry of two coadsorbed CO molecules is also shown in Figure S19. The two CO molecules adsorb next to each other on two bridging Mo atoms and this adsorption geometry is different from that of one CO molecule in that one of the two CO molecules has a twofold adsorption mode with two bridging Mo atoms. Furthermore, the reconstruction of a surface S monomer, similar to that observed for CO_2 adsorption, was found necessary to achieve this coadsorption geometry. Unlike desorption which displays negligible effect of reducing electrode potential, the diffusion is strongly affected by the electrode potential and becomes exothermic at potentials more reducing than -1.7 V. The alternate desorption starting from the coadsorbed structure is more likely, although, it has an opposite effect of electrode potential compared to diffusion process.

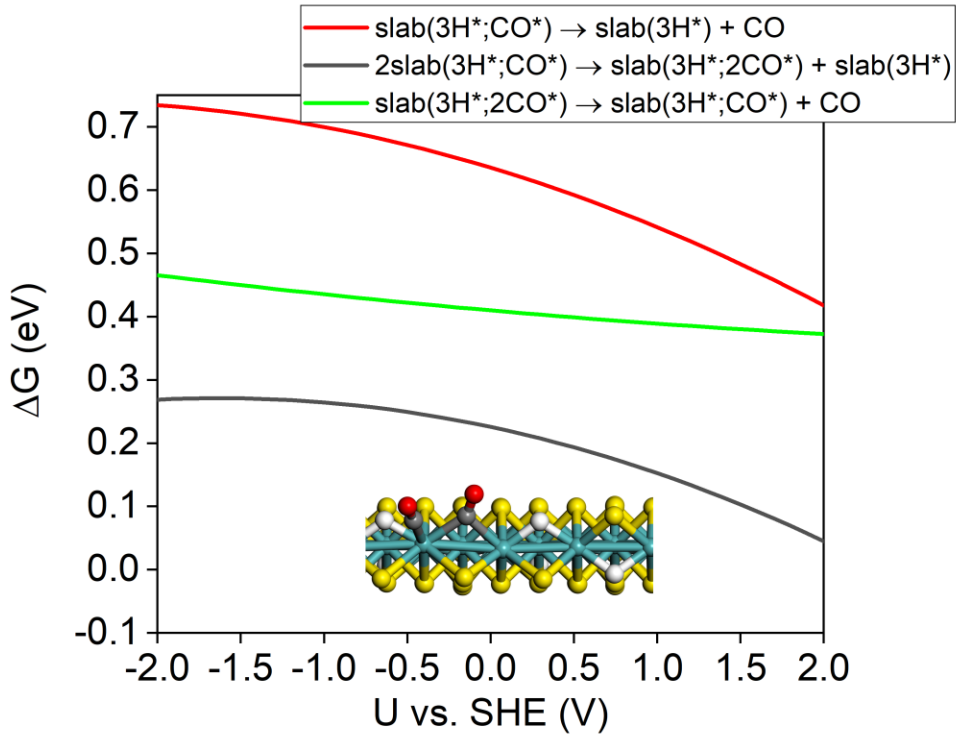

Figure S19: Gibbs free energy change of different chemical transformations involving CO on the S-edge.

References

(S1) Nørskov, J. K.; Rossmeisl, J.; Logadottir, A.; Lindqvist, L.; Kitchin, J. R.; Bligaard, T.; Jónsson, H. Origin of the Overpotential for Oxygen Reduction at a Fuel-Cell Cathode. *The Journal of Physical Chemistry B* **2004**, *108*, 17886–17892.

(S2) Abidi, N.; Bonduelle-Skrzypczak, A.; Steinmann, S. N. How Stable Are 2H-MoS_2 Edges under Hydrogen Evolution Reaction Conditions? *The Journal of Physical Chemistry C* **2021**, *125*, 17058–17067.

(S3) Tsai, C.; Chan, K.; Nørskov, J. K.; Abild-Pedersen, F. Rational design of MoS_2 catalysts: tuning the structure and activity via transition metal doping. *Catal. Sci. Technol.* **2015**, *5*, 246–253.

(S4) Huang, Y.; Nielsen, R. J.; Goddard, W. A., III; Soriaga, M. P. The Reaction Mechanism with Free Energy Barriers for Electrochemical Dihydrogen Evolution on MoS_2. *Journal of the American Chemical Society* **2015**, *137*, 6692–6698.

(S5) Ruffman, C.; Gordon, C. K.; Skúlason, E.; Garden, A. L. Mechanisms and Potential-Dependent Energy Barriers for Hydrogen Evolution on Supported MoS2 Catalysts. *The Journal of Physical Chemistry C* **2020**, *124*, 17015–17026.

(S6) Prodhomme, P.-Y.; Raybaud, P.; Toulhoat, H. Free-energy profiles along reduction pathways of MoS_2 M-edge and S-edge by dihydrogen: A first-principles study. *Journal of Catalysis* **2011**, *280*, 178–195.

(S7) Helveg, S.; Lauritsen, J. V.; Lægsgaard, E.; Stensgaard, I.; Nørskov, J. K.; Clausen, B. S.; Topsøe, H.; Besenbacher, F. Atomic-Scale Structure of Single-Layer MoS_2 Nanoclusters. *Phys. Rev. Lett.* **2000**, *84*, 951–954.

(S8) Thomas F. Jaramillo; Kristina P. Jørgensen; Jacob Bonde; Jane H. Nielsen; Sebastian Horch;

Ib Chorkendorff Identification of Active Edge Sites for Electrochemical H_2 Evolution from MoS_2 Nanocatalysts. *Science (New York, N.Y.)* **2007**, *317*, 100–102.

(S9) Heyd, J.; Scuseria, G. E. Efficient hybrid density functional calculations in solids: Assessment of the Heyd–Scuseria–Ernzerhof screened Coulomb hybrid functional. *The Journal of Chemical Physics* **2004**, *121*, 1187–1192.

(S10) Reaction mechanisms for reduction of CO_2 to CO on monolayer MoS_2. *Applied Surface Science* **2020**, *499*, 143964.